Supporting Information

Ag-Pt Compositional Intermetallics Made from Alloy Nanoparticles

*Yung-Tin Pan[1], Yuqi Yan[1], Yu-Tsun Shao[2], Jian-Min Zuo[2], Hong Yang[1]**

[1]Department of Chemical and Biomolecular Engineering, University of Illinois at Urbana-Champaign, 206 Roger Adam Laboratory, MC-712, 600 South Mathews Avenue, Urbana, IL 61801

[2]Department of Materials Science and Engineering, University of Illinois at Urbana-Champaign, 1006 Materials Research Laboratory, 104 South Goodwin Avenue, Urbana, IL 61801

*: E-mail: hy66@illinois.edu

Materials and Chemicals

Platinum acetylacetonate ($Pt(acac)_2$, 98%) was purchased from Strem Chemicals; silver stearate (99%) from Pfaltz & Bauer; oleylamine (OAm, 70%), oleic acid (OAc, 90%), diphenyl ether (DPE, 99%), 1,2-hexadecanediol (1,2-HDD, 90%), and Nafion 117 solution from Sigma-Aldrich; chloroform (>99%) and methanol (>99%) from Macron; ethanol (200 proof) from Decon Labs; carbon black (Vulcan XC-72) from Cabot; perchloric acid (70%, VERITAS double distilled) and formic acid (88%) from GFS Chemicals; propanol (LC-MS Reagent) from J. T. Baker; Pt/C catalyst (20% Pt on Vulcan XC-72) from BASF; argon gas (Ar, UHP grade) from Airgas; and nitrogen gas (C.P grade) from S J Smith. All chemicals were used as received without further purification.

Synthesis and Processing of Ag_xPt_y Nanoparticles

Ag_xPt_y alloy nanoparticles were synthesized through a wet chemical route. In a typical synthesis, designed amount of $Pt(acac)_2$ and Ag stearate (total of 0.191 mmol), 490 mg of 1,2-hexadecanediol (1,2-HDD 1.9 mmol), 0.3 mL of oleylamine, 0.3 mL of oleic acid, and 5 mL of diphenyl ether were mixed in a 15-mL three-neck round-bottom flask. The flask was connected to a Schlenk line through a condenser. The reaction mixture was preheated at 55 °C until metal precursors and 1,2-HDD were completely dissolved to form a homogeneous orange color solution. The flask was then evacuated with a rotary pump (Edward RV 12) and purged with Ar for six cycles. The temperature of the solution was ramped at a rate of 5 °C/min to 260 °C, maintained for 1 h, and then cooled down to room temperature under Ar. The solid products were collected by centrifugation where ethanol was added into the synthesis solution to dissolve excess 1,2-HDD. The nanoparticles were

re-dispersed in chloroform with ultra-sonication and separated from solvents by centrifugation in a chloroform-ethanol mixture at 7000 rpm. This process was repeated two times. The final products were dispersed in chloroform for further characterization. Thermal treatment was carried out in a tube furnace (Lindburg Blue M, Thermo Scientific) with a quartz tube. The dry powders of nanoparticles were introduced into the tube furnace in an alumina boat. The heat treatment was conducted under N_2 atmosphere at 700 °C for 1 h with a ramp rate of 5 ºC/min and then cooled down naturally. The nanoparticles were sintered and converted after this process.

Characterization

Powder X-ray diffraction (XRD) patterns were acquired on a Bruker D8 Venture diffractometer. Transmission electron microscopy (TEM) and high-resolution transmission electron microscopy (HR-TEM) micrographs were taken on a JEOL 2100 Cryo TEM with an accelerating voltage of 200 kV. High angle annular dark field scanning transmission electron microscopy (HAADF-STEM) micrographs were carried out on JEOL 2200 FS STEM with Schottky field emitter and a spherical aberration corrector (Cs-corrector) at an accelerating voltage of 200 kV. Scanning electron microscopy (SEM) and energy dispersive X-ray was performed on Hitachi S4700 SEM. X-ray photoelectron spectroscopy (XPS) data were acquired using PHI 5400 XPS (Physical Electronics) spectrometer with a Mg source. The analysis of XPS spectra was done using CasaXPS software with Shirley type baseline.

Electrochemical Characterization

Electrochemical properties of Ag-Pt catalysts were characterized in a three-electrode cell. To prepare a working electrode, Ag-Pt particles were dispersed in an ethanol/water mixture (with 1:1 volumetric ratio) at a concentration of 3.4 mg/mL. A total of 30 μL was drop-cast onto the glassy-carbon rotating disk electrode (RDE, area: 0.196 cm^2). After deposition of Ag-Pt particles, a drop of Nafion solution (10 μL, diluted by five times from the supplier with ethanol) was drop-cast onto the RDE. A platinum foil (1 cm^2) was used as the counter electrode and a HydroFlex hydrogen electrode as the reference. Hydrogen evolution reaction (HER) was used to calibrate the hydrogen electrode before the tests. The electrochemical active surface area (ECSA), based on proton adsorption on Pt, was carried out by cyclic voltammetry (CV) under Ar saturated 0.1-M perchloric acid ($HClO_4$) and was determined by integrating the area accounted for proton adsorption in the potential range of 0.05-0.4V (vs RHE) with the following formula:

$$\text{ECSA } (cm^2_{Pt}) = \text{area}/[0.05\ (V/s) \times 210\ (\mu C/cm^2)]$$

Oxidation of formic acid was carried out in a mixture of 0.5-M formic acid (HCOOH) and 0.1-M $HClO_4$ by CV under Ar where the area specific activity was derived by normalizing the oxidation current by the ECSA. Data were used without *iR*-drop correction.

Density Functional Theory (DFT) Calculation

DFT calculation was performed using the CASTEP module with ultrasoft pseudopotentials.[1] The electron exchange and correlation energy was treated with generalized gradient approximation (GGA) and with the Perdew−Burke−Ernzerhof (PBE) functional using Tkatchenko-Scheffler (TS)

dispersion correction.[2, 3, 4] The plane-wave basis set cut-off energy was set to 300 eV. The bulk energy of Ag and Pt was calculated based on a face-centered cubic unit cell whereas the cubic closely-packed (CCP) intermetallic was based on a cubic unit cell of 32 atoms and the hexagonal closely-packed (HCP) intermetallic was based on a hexagonal unit cell with 16 atoms. The slab energy for Ag and Pt (111} surfaces was calculated based on a slab with 12 atoms (1×1, 3 layers, 10 Å vacuum). The slab energy for CCP intermetallic (111) surface was calculated based on a slab with 96 atoms (1×1, 3 layers, 10 Å vacuum). The slab energy for HCP intermetallic (001) surface was calculated based on a slab with 96 atoms (2×2, 1 layer, 10 Å vacuum). The Monkhorst-Pack scheme k-point grid sampling was set to 3×4×1 for the surface. The tolerance for convergence was 1×10^{-5} eV/atom in energy, 3×10^{-2} eV/Å in force, and 1×10^{-3} Å in displacement. The surface energy was calculated using the following equation:[5]

$$\sigma = [E_{slab} - (N_{slab}/N_{bulk})E_{bulk}]/2N_{slab}$$

where σ is the surface energy per atom, E_{slab} is the total energy of the created metal surface, E_{bulk} is the total energy of the bulk metal, N_{slab} is the number of atoms in the created metal surface, and N_{bulk} is the number of atoms in the unit cell.

DIFFaX Simulation of X-Ray Diffraction Patterns

Simulation of X-ray diffraction pattern was conducted with the DIFFaX program which is designed for calculating diffraction intensity for crystals that contain planar defects, such as twins and stacking faults.[6] The simulation was built on a deformed hexagonal unit cell and the grain dimensions along three directions were assigned to reflect preferential orientation. Four different layers of closed-packed Pt and Ag were created to construct the stacks along *c*-axis either on the

tetrahedral or octahedral sites, in which the probability of each layer stacking on one another can be assigned. Ag-Pt CCP and HCP intermetallics without preferential orientation were simulated by building a hexagonal unit cell with alternating Ag and Pt layers. The DIFFaX structure data files for simulating the powder pattern of compositional intermetallic with faulted structures are listed as follows:

Structure data file for the compositional intermetallic

```
{data file for AgPt, with layer Ag on layer Pt interchangeably}
{probability of hexagonal stacking = 85%}

INSTRUMENTAL                          {Header for instrumental section}
X-RAY                                 {Simulate X-ray diffraction}
1.5418                                {X-ray wavelength}
PSEUDO-VOIGT 0.1 -0.036 0.009 0.6 trim {Instrumental broadening}

STRUCTURAL                            {Header for structural section}
2.67 2.80 2.38 120.0                  {unit cell coordinates}
Unknown                               {hexagonal, c axis = cubic [111]}
4                                     {111 sheet, plus its mirror}
1050    42                            {layer widths very wide in the a-b plane}

LAYER 1                               {cubic (111) layer, centrosymmetric}
CENTROSYMMETRIC
Pt    1  0.0   0.0   0.0  0.2   1.0  {name id# x_rel y_rel z_rel B_iso Occ}
                                      {B_iso = isotropic Debye-Waller factor}
                                      {Occ= occupancy factor}

LAYER 2
CENTROSYMMETRIC
Ag    1  0.0   0.0   0.0  0.2   1.0

LAYER 3
CENTROSYMMETRIC
Pt    1  0.0   0.0   0.0  0.2   1.0

LAYER 4
CENTROSYMMETRIC
Ag    1  0.0   0.0   0.0  0.2   1.0


STACKING                              {Header for stacking description}
recursive                             {Statistical ensemble}
100                                   {Infinite number of layers}

TRANSITIONS                           {Header for transitions}
{Transitions from layer 1}
0.01    1/3  2/3   1.0                {layer 1 to layer 1, 1%   chance}
0.99    1/3  2/3   1.0                {layer 1 to layer 2, 99% chance}
0.0     2/3  1/3   1.0                {layer 1 to layer 3, 0 %  chance}
0.0     2/3  1/3   1.0                {layer 1 to layer 4, 0%   chance}


{Transitions from layer 2}
0.145    1/3  2/3   1.0               {layer 2 to layer 1, 14.5%  chance}
0.005    1/3  2/3   1.0               {layer 2 to layer 2, 0.5%   chance}
0.845    2/3  1/3   1.0               {layer 2 to layer 3, 84.5%  chance}
0.005    2/3  1/3   1.0               {layer 2 to layer 4, 0.5%   chance}


{Transitions from layer 3}
0.005    1/3  2/3   1.0               {layer 3 to layer 1, 0.5%   chance}
0.495    1/3  2/3   1.0               {layer 3 to layer 2, 49.5%  chance}
0.005    2/3  1/3   1.0               {layer 3 to layer 3, 0.5%   chance}
0.495    2/3  1/3   1.0               {layer 3 to layer 4, 49.5%  chance}


{Transitions from layer 4}
0.495   1/3  2/3    1.0               {layer 4 to layer 1, 49.5%  chance}
0.005   1/3  2/3    1.0               {layer 4 to layer 2, 0.5%   chance}
0.495   2/3  1/3    1.0               {layer 4 to layer 3, 49.5%  chance}
0.005   2/3  1/3    1.0               {layer 4 to layer 4, 0.5%   chance}
```

Structure data file for intermetallic stacking in hcp structure

{data file for AgPt, with Ag layer on Pt layer interchangeably with hexagonal stacking}

```
INSTRUMENTAL                          {Header for instrumental section}
X-RAY                                 {Simulate X-ray diffraction}
1.5418                                {X-ray wavelength}
PSEUDO-VOIGT 0.1 -0.036 0.009 0.6 trim {Instrumental broadening}

STRUCTURAL                            {Header for structural section}
2.715 2.715 2.38 120.0                {unit cell coordinates}
unknown                               {hexagonal, c axis = cubic [111]}
2                                     {111 sheet, plus its mirror}
100  100                              {layer widths very wide in the a-b plane}

LAYER 1                               {cubic (111) layer, centrosymmetric}
CENTROSYMMETRIC
Pt    1  0.0   0.0   0.0  0.2   1.0  {name id# x_rel y_rel z_rel B_iso Occ}
                                      {B_iso = isotropic Debye-Waller factor}
                                      {Occ= occupancy factor}
LAYER 2
CENTROSYMMETRIC
Ag    1  0.0   0.0   0.0  0.2   1.0

STACKING                              {Header for stacking description}
recursive                             {Statistical ensemble}
700                                   {# of layers }

TRANSITIONS                           {Header for transitions}
{Transitions from layer 1}
0.0    1/3  2/3   1.0                 {layer 1 to layer 1, 0%    chance}
1.0    1/3  2/3   1.0                 {layer 1 to layer 2, 100% chance}

{Transitions from layer 2}
1.0    -1/3  -2/3   1.0               {layer 2 to layer 1, 100%  chance}
0.0    1/3  2/3   1.0                 {layer 2 to layer 2, 0%      chance}
```

Structure data file for intermetallic stacking in fcc structure

```
{data file for AgPt, with Ag layer on Pt layer interchangeably with CCP stacking}

INSTRUMENTAL                          {Header for instrumental section}
X-RAY                                 {Simulate X-ray diffraction}
1.5418                                {X-ray wavelength}
PSEUDO-VOIGT 0.1 -0.036 0.009 0.6 trim {Instrumental broadening}

STRUCTURAL                            {Header for structural section}
2.715 2.715 2.38 120.0                {unit cell coordinates}
unknown                               {hexagonal, c axis = cubic [111]}
2                                     {111 sheet, plus its mirror}
500  500                              {layer widths very wide in the a-b plane}

LAYER 1                               {cubic (111) layer, centrosymmetric}
CENTROSYMMETRIC
Pt    1  0.0   0.0   0.0  0.2   1.0  {name id# x_rel y_rel z_rel B_iso Occ}
                                      {B_iso = isotropic Debye-Waller factor}
                                      {Occ= occupancy factor}

LAYER 2
CENTROSYMMETRIC
Ag    1  0.0   0.0   0.0  0.2   1.0


STACKING                              {Header for stacking description}
recursive                             {Statistical ensemble}
500                                   {Infinite number of layers}

TRANSITIONS                           {Header for transitions}
{Transitions from layer 1}
0.0    1/3  2/3   1.0                 {layer 1 to layer 1, 0%    chance}
1.0    1/3  2/3   1.0                 {layer 1 to layer 2,100% chance}

{Transitions from layer 2}
1.0    1/3  2/3   1.0                 {layer 2 to layer 1, 100%  chance}
0.0    1/3  2/3   1.0                 {layer 2 to layer 2, 0%      chance}
```

Table S1. Analysis of surface composition using XPS

Entry		1	2	3	4
Composition	nominal	$Ag_{53}Pt_{47}$	$Ag_{50}Pt_{50}$	$A_{48.4}Pt_{51.6}$	$Ag_{47}Pt_{53}$
	XPS analysis	$Ag_{69}Pt_{31}$	$Ag_{68}Pt_{32}$	$Ag_{67}Pt_{33}$	$Ag_{52}Pt_{48}$

Table S2. Analysis of composition of the sintered $Ag_{48.4}Pt_{51.6}$ catalysts before and after formic acid oxidation (FAOR) using EDX and XPS

	Composition	
	SEM-EDX	XPS
Prior to FAOR	$Ag_{57}Pt_{43}$	$Ag_{67}Pt_{33}$
After FAOR	$Ag_{53}Pt_{47}$	$Ag_{49}Pt_{51}$

Table S3. Integrated area and calculated ECSA based on the CV measurements*

	as-made	intermetallic	Pt/C
area (w)	3.13×10^{-5}	5.23×10^{-6}	5.50×10^{-5}
ECSA (cm^2)	2.98	0.498	5.24

*: The ECSA values were obtained based on the integrated area between 0.05 and 0.4V for proton adsorption.

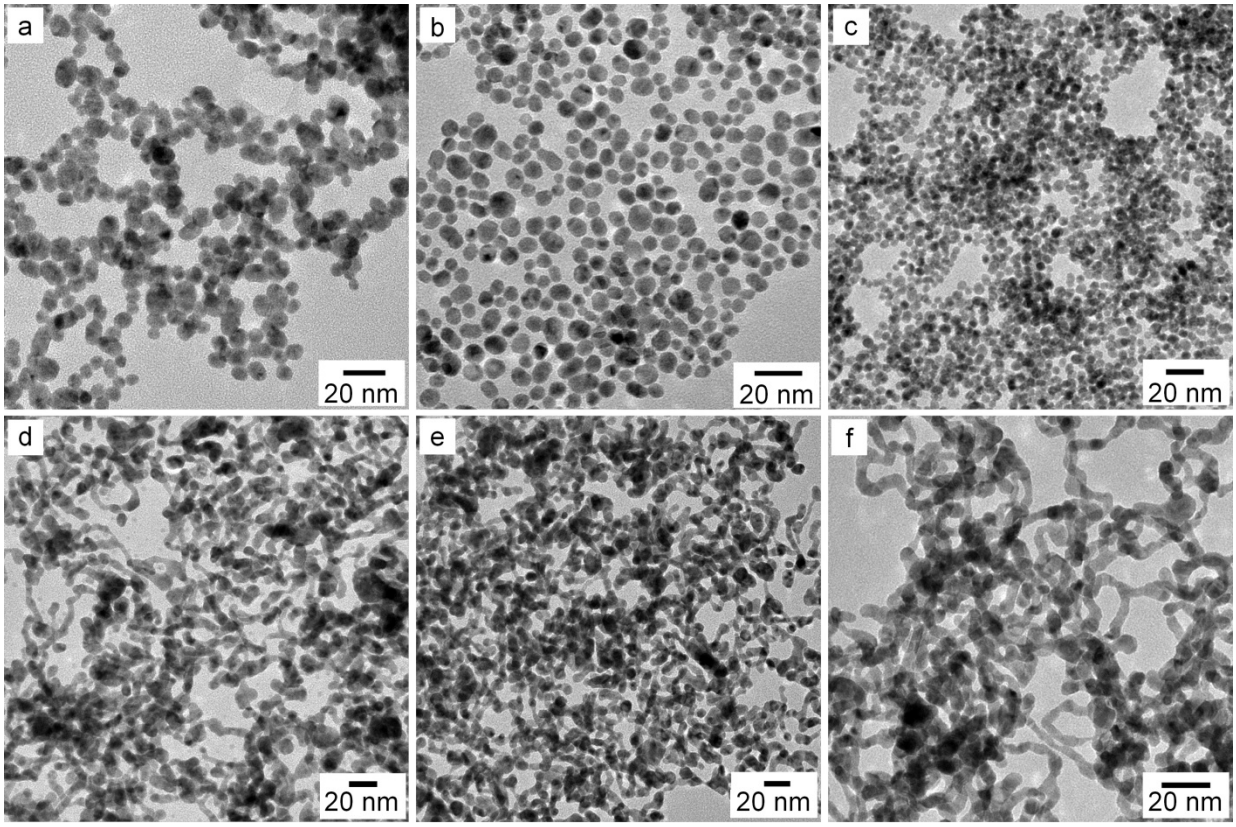

Figure S1. TEM micrographs of as-made Ag-Pt alloy nanoparticles at the nominal composition of (a) $Ag_{75}Pt_{25}$, (b) $Ag_{60}Pt_{40}$, (c) $A_{53}Pt_{47}$, (d) $Ag_{48.4}Pt_{51.6}$, (e) $Ag_{47}Pt_{53}$, and (f) $Ag_{33}Pt_{67}$, respectively.

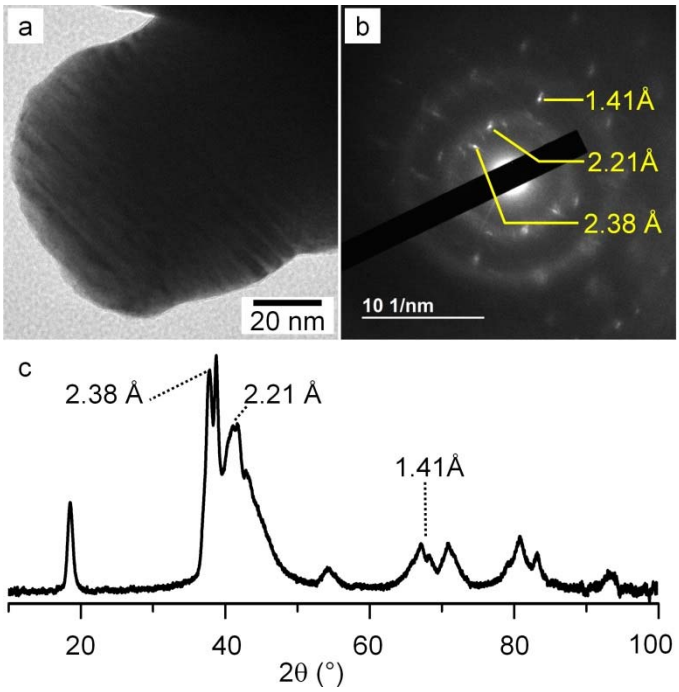

Figure S2. (a) Bright field TEM, (b) selected area electron diffraction (SAED) and (c) PXRD of thermally treated $Ag_{48.4}Pt_{51.6}$ sample. The highlighted SAED spots could be correlated to specific diffraction peaks labeled in the PXRD pattern.

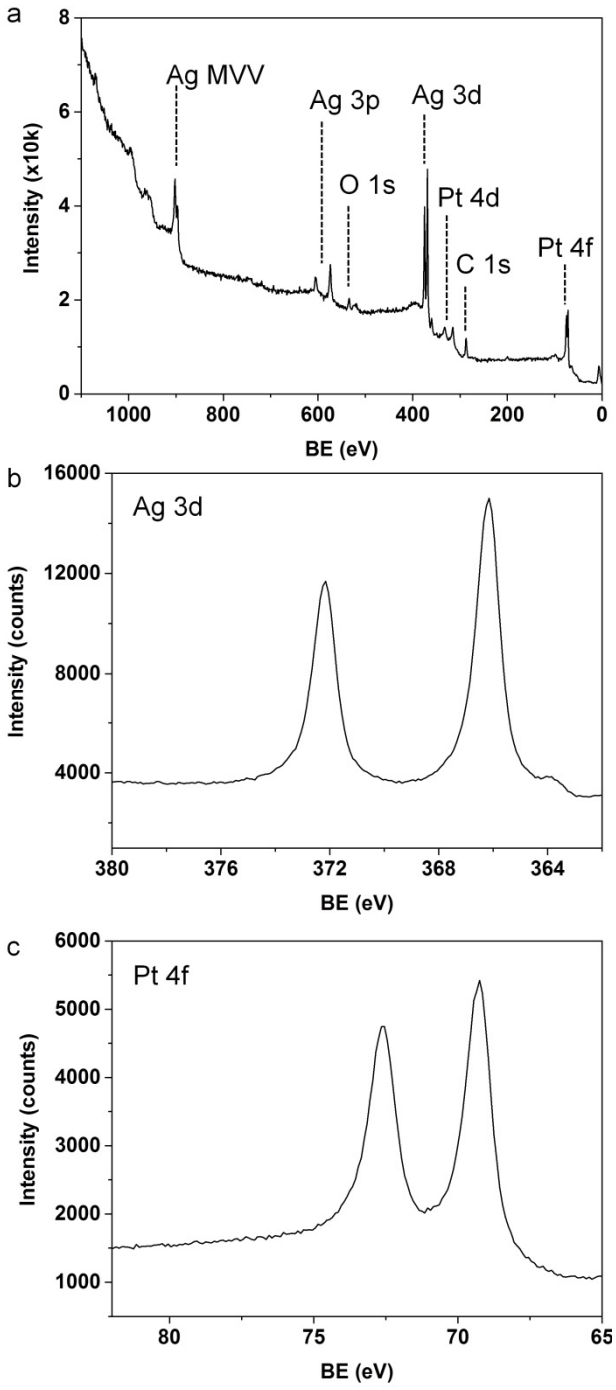

Figure S3. XPS spectra of the thermally treated $A_{53}Pt_{47}$ sample: (a) survey scan, (b) Ag 3d, and (c) Pt 4f regions.

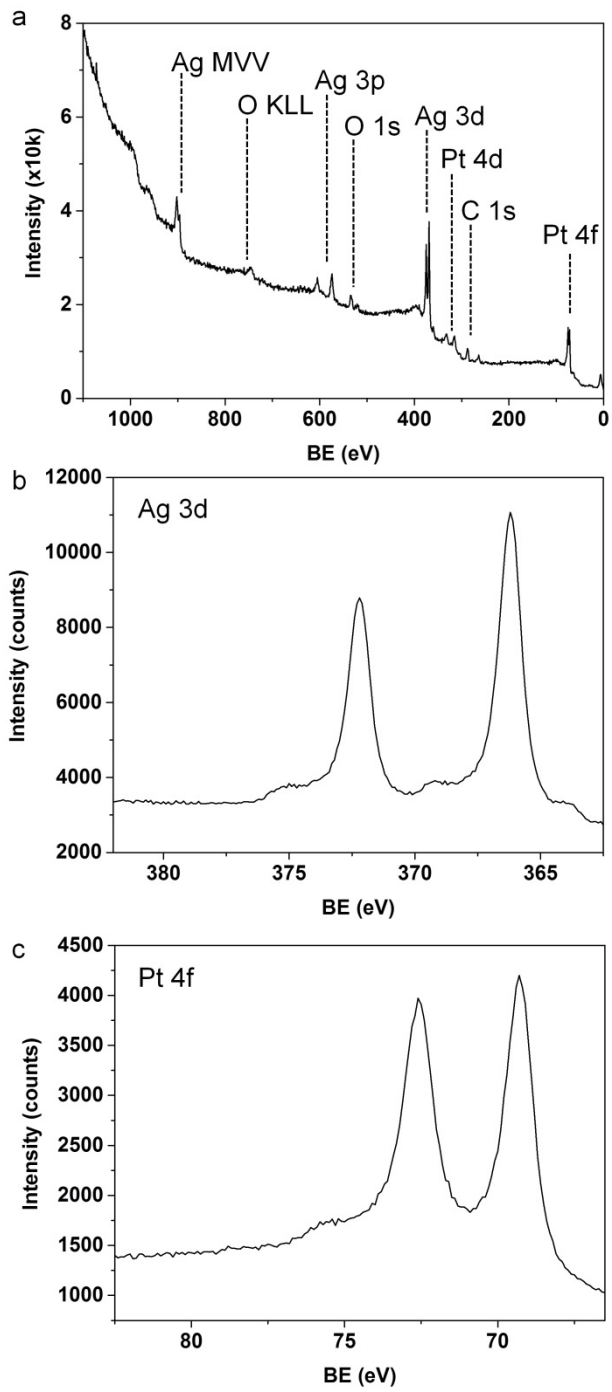

Figure S4. XPS spectra of the thermally treated $Ag_{50}Pt_{50}$ sample: (a) survey scan, (b) Ag 3d, and (c) Pt 4f regions.

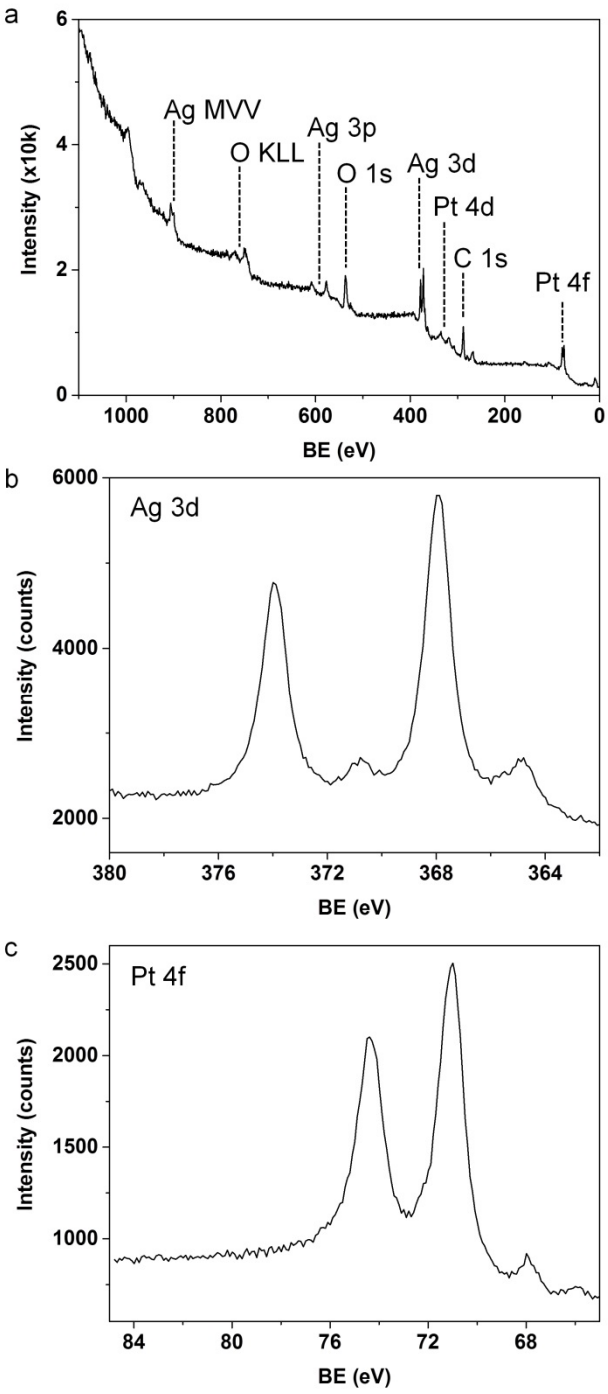

Figure S5. XPS spectra of the thermally treated $Ag_{48.4}Pt_{51.6}$ sample: (a) survey scan, (b) Ag 3d, and (c) Pt 4f regions.

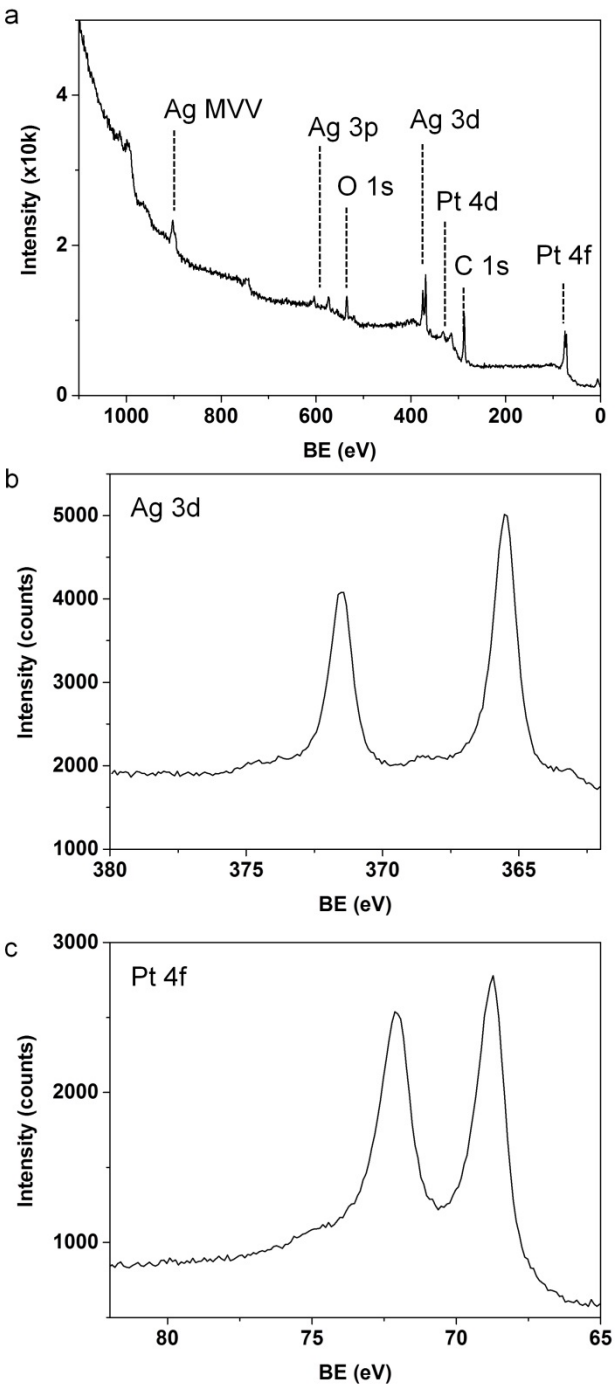

Figure S6. XPS spectra of the thermally treated $Ag_{47}Pt_{53}$ sample: (a) survey scan, (b) Ag 3d, and (c) Pt 4f regions.

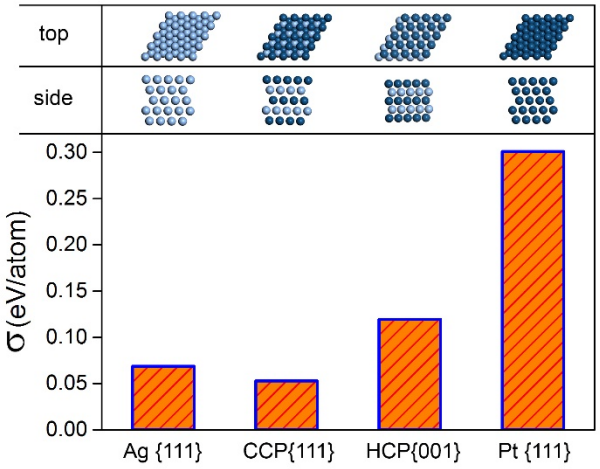

Figure S7. Surface energy of Ag, Pt, Ag-Pt CCP, and Ag-Pt HCP intermetallics obtained by DFT calculation.

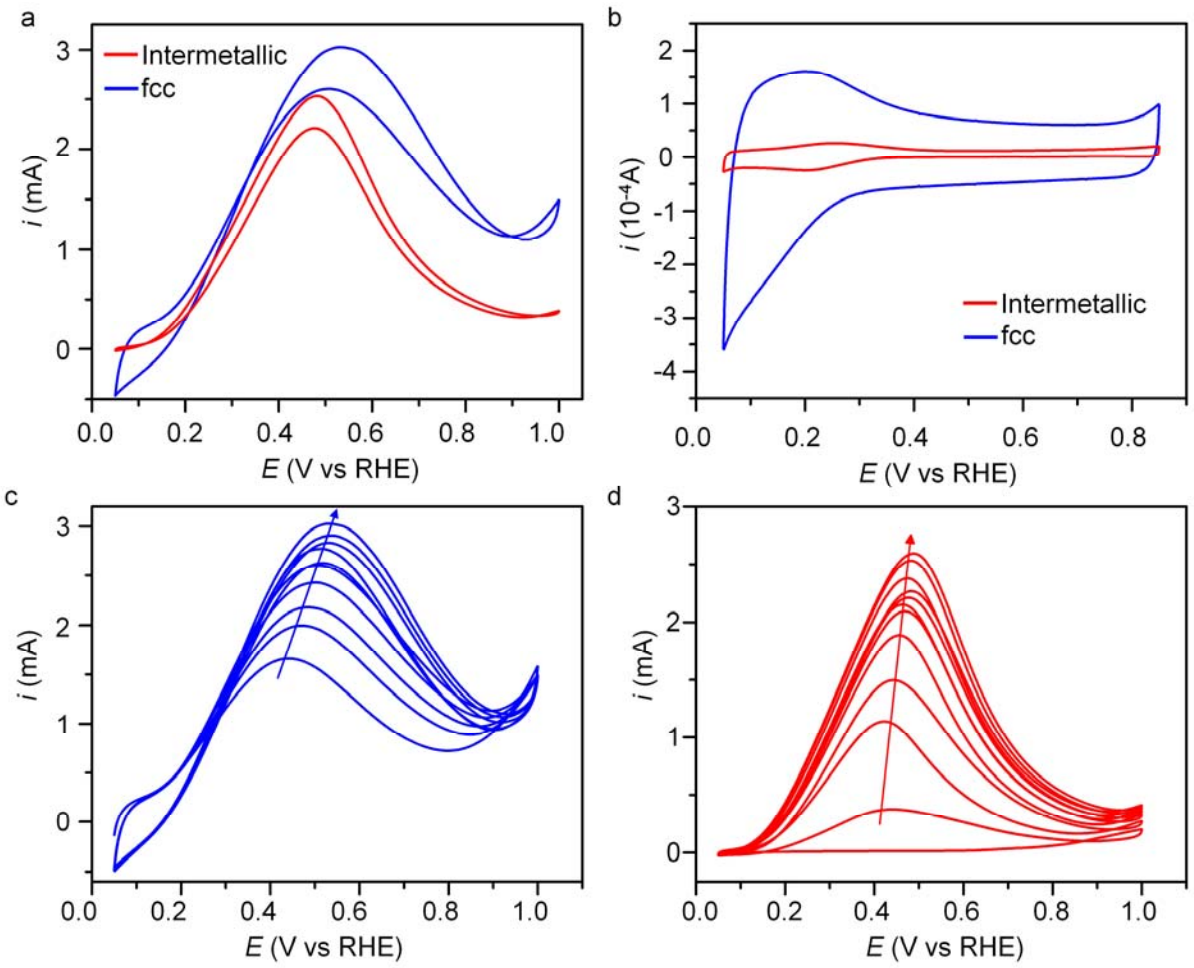

Figure S8. CV curves showing the electrocatalytic performance towards formic acid oxidation reaction (FAOR) by the intermetallic and fcc random alloy nanoparticle catalysts with a nominal composition of $Ag_{48.4}Pt_{51.6}$. (a) Stable CV curves measured in Ar-saturated solution of 0.5-M HCOOH and 0.1-M $HClO_4$ for the 5th cycle, (b) CV curves measured in Ar-saturated 0.1-M $HClO_4$ solution for ECSA analysis. The change of the initial five CV cycles for FAOR catalyzed by Ag-Pt (c) alloy nanoparticles and (d) compositional intermetallics.

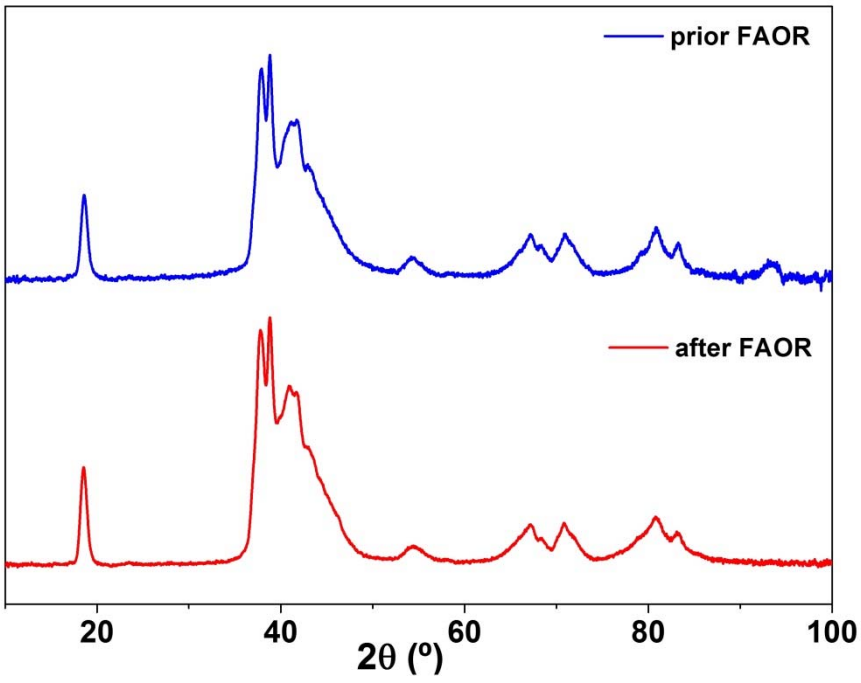

Figure S9. Powder XRD patterns of the compositional intermetallic catalyst before and after FAOR tests. (Nominal composition was $Ag_{48.4}Pt_{51.6}$)

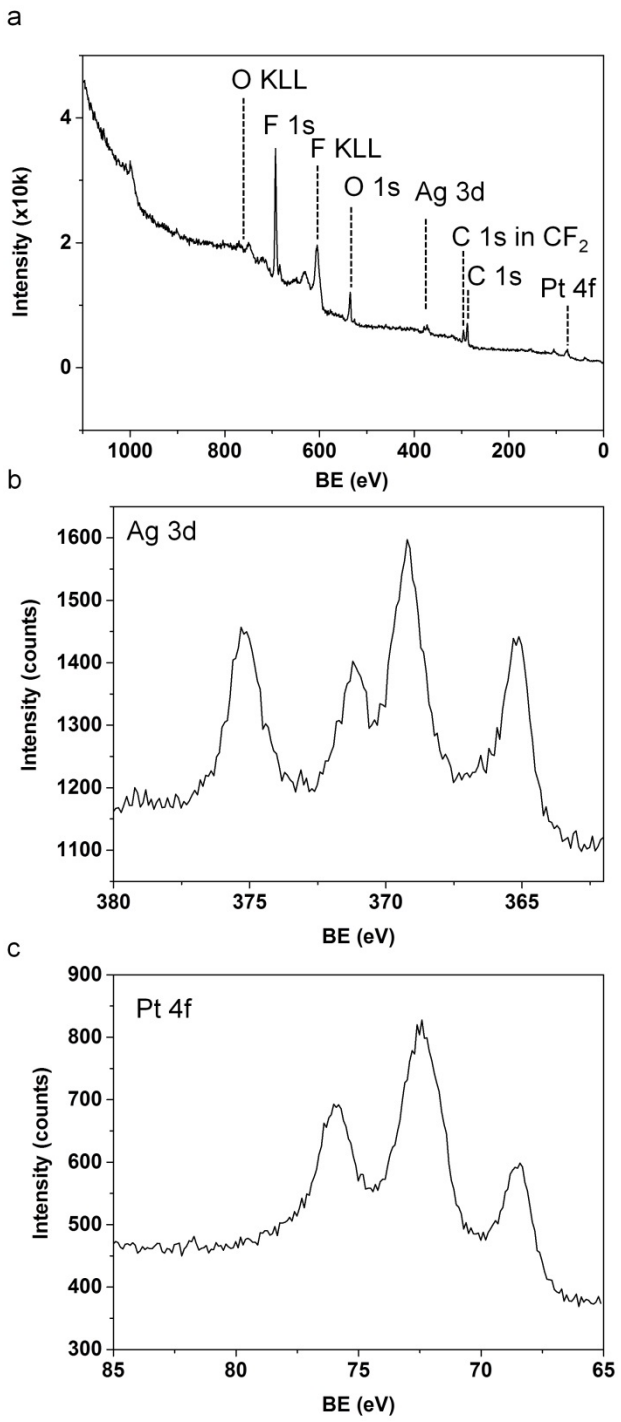

Figure S10. XPS spectra of thermally treated $Ag_{48.4}Pt_{51.6}$fter FAOR test. (a) Survey scan, (b) Ag 3d, and (c) Pt 4f regions. The extra peaks for the Ag 3d and Pt 4f regions were due to charging from the Nafion coating.

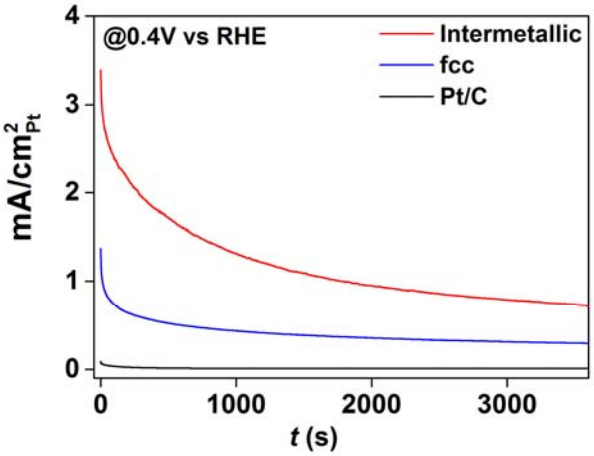

Figure S11. Chronoamperometric anodic currents for formic acid oxidation for Ag-Pt intermetallic and fcc random alloy, and the reference Pt/C catalyst at 0.4 V vs RHE.

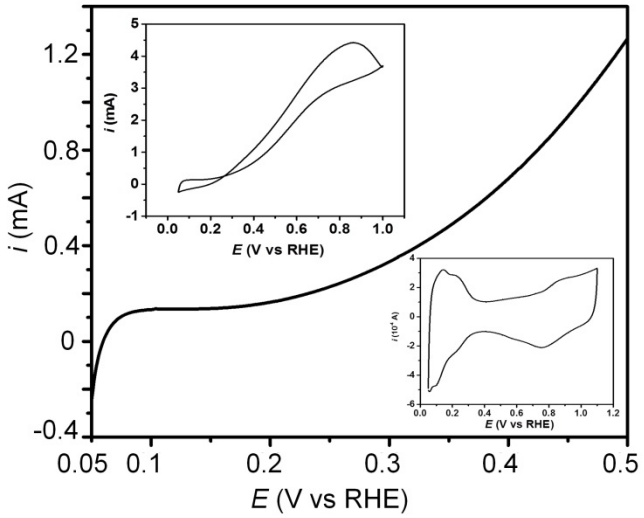

Figure S12. FAOR catalyzed by reference Pt/C catalyst. Inset at the upper left shows the full CV scan for FAOR from 0.05 to 1.0 V and inset at the lower right the proton adsorption/desorption in 0.1-M $HClO_4$ solution.

REFERENCE

1. Clark Stewart, J.; Segall Matthew, D.; Pickard Chris, J.; Hasnip Phil, J.; Probert Matt, I. J.; Refson, K.; Payne Mike, C. *Kristallogr.* **2005,** *220*, 567-570.
2. Armbrüster, M.; Kovnir, K.; Behrens, M.; Teschner, D.; Grin, Y.; Schlögl, R. *J. Am. Chem. Soc.* **2010,** *132*, 14745-14747.
3. Tkatchenko, A.; Scheffler, M. *Phys. Rev. Lett.* **2009,** *102*, 073005.
4. Yin, X.; Liu, X.; Pan, Y.-T.; Walsh, K. A.; Yang, H. *Nano Lett.* **2014,** *14*, 7188-7194.
5. Methfessel, M.; Hennig, D.; Scheffler, M. *Phys. Rev. B* **1992,** *46*, 4816-4829.
6. Treacy, M. M. J.; Newsam, J. M.; Deem, M. W. *P. Roy. Soc. Lond. A Mat.* **1991,** *433*, 499-520.